

Development of technology for manufacturing NbN HEB mixers with a small spread of DC and RF parameters for the creation of matrix receivers in the terahertz range

© I.V. Tretyakov,¹ N.S. Kaurova,² I.V. Ivashenceva,² B.M. Voronov,² G.N. Goltsman^{2,3}

¹Astro Space Center of P.N. Lebedev Physical Institute of the Russian Academy of Sciences
117997 Moscow, Russia

²Moscow Pedagogical State University,
119435 Moscow, Russia

³National Research University Higher School of Economics,
101000 Moscow, Russia
e-mail: ivantretykov@mail.ru

Received May 16, 2024

Revised May 16, 2024

Accepted May 16, 2024

The work is devoted to an experimental study of the influence of the process parameters of magnetron deposition of a thin 4–5 nm superconducting film of niobium nitride NbN and the fabrication technology of NbN HEB mixers on the spread of their main parameters to minimize this spread in the future. The main parameters of the NbN HEB mixer are normal resistance R_{300} , critical temperature T_c , superconducting transition width T_c , noise temperature T_n , conversion bandwidth B and required local oscillator power P_{obs} . Studies of B and current-voltage IV characteristics of NbN HEB mixers were carried out at different temperatures of the Si substrate, at T near T_c and T much lower than T_c , this made it possible to identify individual interfaces in the mixer due to their different T_c and study their influence. The uniformity of parameters of NbN HEB mixers, in addition to optimizing the NbN film deposition process, was achieved by preparing the surface of the Si substrate, as well as by using an Au layer deposited *in situ* with the NbN film — contact with a planar THz antenna. The NbN HEB mixers manufactured according to the optimized route had almost identical $R(T)$ characteristics with a spread of T_c and normal resistance R_{300} of no more than 0.15 K and $2\ \Omega$, respectively. The noise temperature at the local oscillator frequency of 2.52 THz was 800 K with a variation of 150 K from device to device. The noise bandwidth of the mixers at $T = 4.5$ K averaged 7 GHz. Optimized fabrication technology will make it possible in the future to create multi-pixel heterodyne arrays from NbN HEB mixers with high uniformity of pixel parameters.

Keywords: terahertz range, thin film niobium nitride, heterodyne receiver.

DOI: 10.61011/TP.2024.07.58807.174-24

Introduction

With the development of instrumentation, submillimetric and terahertz electromagnetic radiation bands occurred to be available for spectroscopic observations. These bands contain spectral lines of chemical compounds important for medical applications, security and control systems, environment, cosmology, planetary astronomy and other areas such as C^+ , CO, CH, CH^+ , CH_3D , HCN, HNC, O_2 , HCl, HF, Cl, OH, OH^+ , MgH, H_2O , O_3 lines.

When an observed spectral line is found to belong to a „spectral signature“ of any compounds, then, according to its intensity, the abundance of this compound and the processes flowing in the observed space area may be assessed. For example, C^+ ($158\ \mu m$) line is more bright in the submillimetric Milky Way radiation spectrum suggesting high abundance of this element in the galaxy. The intensity of this line define the star formation regions where the surrounding dust accumulations are heated very much by the ultraviolet radiation [1].

Considerable progress in the submillimetric band spectroscopy was provided by the development of low-noise mixers on the superconductor–insulator–superconductor (SIS) tunnel junction [2,3]. The noise temperature of SIS receivers is only a few times higher than the quantum limit, however, increases dramatically at heterodyne frequencies higher than the gap frequency for the superconductor to be used (700 GHz for Nb). The maximum heterodyne frequency at which operation of SIS mixers based on NbTiN films was demonstrated is 1.4 THz [4]. At frequencies higher than 1 THz, a hot electron superconductor mixer — hot electron bolometer (HEB) has the highest sensitivity and requires a lower heterodyne power level. Heterodyne source for frequencies higher than 1 THz is an intrinsically sophisticated device consisting of a heterodyne and a phase and frequency stabilization system. The width of the heterodyne line defines the receiver frequency resolution. Currently, the existing instruments use Schottky barrier diode multipliers, quantum-cascade lasers, photoconductive antennas and UTC diodes (uni-revealing carriers diode) as

a generator. Thus, the noise temperature measured in the two-band mode reached 650 K at the heterodyne frequency of 2.5 THz for HEB mixers [5].

Due to high sensitivity of HEB mixers they are used in astronomic projects of the European Space Agency: SOFIA Stratospheric Observatory with the 2.5 meter mirror designed to conduct observations at frequencies from 1 to 5 THz, [6] and TELIS [2] for operation within 1.76–1.86 THz. The HERSCHEL space observatory also used HEB mixers in 1.4–1.9 THz channel [7]. Among the SOFIA instruments, 1.4, 1.9 and 2.5 THz channels of the GREAT instrument are based on single waveguide NbN HEB mixers [8]. The upGREAT instrument, GREAT receiver, is already a multipixel heterodyne matrix [9]. The upGREAT low-frequency array (LFA) consists of waveguide HEB 2×7 pixels, two sets are required to separated polarizations at 1.9–2.5 THz. The upGREAT high-frequency array (HFA) consists of 7 waveguide HEB set to operation at 4.745 THz. The hexagonal configuration was chosen to ensure the maximum display efficiency. LFA with a noise temperature of 600 K in the center of the frequency range has been successfully put into operation for observation of CII 1.905 THz line. [6].

The DOME A observatory developed by the Purple Mountain Observatory of the Chinese Academy of Sciences may become a most promising land-based observing station for THz astronomy [10]. China plans to build the DATE5 5 meter THz telescope equipped with two-range heterodyne receiver for the atmospheric window frequencies of 0.85 and 1.4 THz based on the HEB mixers.

The „Millimetron“ [11] project created by the Astro Space Center of P.N. Lebedev Physical Institute of the Russian Academy of Sciences is the sixth space telescope after the ISO, SWAS, Odin, Spitzer and Herschel observatories that provides the opportunity observations at frequencies higher than 0.5 THz. The „Millimetron“ will investigate water origin and transport processes in the Universe — this is one of the key research objective of the observatory [12]. As a result, water content in various space objects from galaxies to comets will be studied, water transport mechanisms between various types of space objects and relation of interstellar water molecules to the origin of life on Earth.

The investigation of water origin and transport in the Universe will be possible by the „Millimetron“ observatory due to single-mirror observations using the „High-Resolution Spectrometer“. This instrument includes heterodyne receivers for the following frequency bands: 500–600 GHz (M1), 750–900 GHz (M2), 1080–1230 GHz (M3), 1300–1400 GHz (M4), 1900 GHz (M5), 2400 GHz (M6), 2600 GHz (M7) [11]. Frequency division considers the existing technological capabilities for creation of receivers.

For M4–M7 ranges operating at frequencies higher than 1.3 THz, heterodyne seven-pixel matrix receivers based on NbN HEB mixers will be used [11]. Terahertz HEB mixers

use the disordered ultrathin (3.5–5 nm) NbN superconductor film as a sensitive element. Currently, each heterodyne matrix pixel — HEB mixer — is considered as a separate detector requiring individual bias voltage and heterodyne power settings. For matrix sizes equal to at least a dozen of pixels, such individual approach to matrix setting is almost not applicable. The problem may be solved by standardized HEB mixers that require no individual setting. For this, NbN film deposition and Si-substrate NbN HEB mixer production technologies shall be improved. Detectors with maximum close $R(T)$ and minimum spread of normal resistances R_{300} at room temperature shall be manufactured for detectors with identical geometry within a single batch.

Moreover, the modern HEB as heterodyne detectors have almost achieved their sensitivity limit [13,14], however, they have a conversion bandwidth not exceeding 3 – 4 GHz [15]. Further reduction of the noise temperature, required heterodyne power and increase in the conversion bandwidth of the NbN HEB mixer are of high practical interest. Physical phenomena that define the operation of a mixer based on the electronic heating effect in superconductor theoretically make it possible to implement a mixer with noise temperature close to the quantum limit and intermediate frequency band much larger than that developed by the moment because the energy relaxation time of excited electrons is very short and this potentially allows a mixer with conversion bandwidth more than 10 GHz to be created on the basis of ultrathin NbN film. However, the mixer response rate is defined by the time of departure of non-equilibrium phonons into the substrate, therefore, to achieve such response rate, this time shall be reduced and conditions for diffusion cooling of the electronic subsystem of the films shall be provided.

Besides the investigation of objects in cold low-radiation areas of the distant Universe, the heterodyne receipt circuit used for submillimetric and terahertz frequency ranges with high spectral resolution also provides unique opportunities for quick non-destructive identification of a substance with extremely low concentrations. In addition, the scope of application of such instruments includes the terahertz microscopy, study of semiconductor emitters, security systems, medicine, etc. To observe narrow nearby weak lines (signals) from fast flowing processes, high-sensitive and fast receivers are primarily required. At frequencies higher than 1.3 THz, only HEB mixers based on ultrathin NbN films ensure the required sensitivity.

1. Manufacturing process

The key aspects of the process compared with those described previously in [5,6] included a special Si substrate surface preparation process, besides the optimization of the NbN film deposition by critical temperature T_c and film thickness h . This process allowed to obtain NbN film with homogeneous thickness. *in situ* deposition of 20 nm Au layer with the NbN film for formation of the THz

Table 1. Stages of quasi-optical NbN HEB mixer manufacturing process shown in Figure 1

Stage	Stage content
<i>a</i> structure	<i>In situ</i> application of two-layer NbN-Au by the reactive magnetron sputtering method
<i>b</i>	Manufacturing alignment marks for photo and electronic lithography
<i>c</i>	Gap formation in Au by the electron-beam lithography method, ionic and chemical etching method
<i>d</i>	Formation of spiral antenna interior by the electron-beam lithography method
<i>e</i>	Formation of spiral antenna exterior by the photolithography method
<i>f</i>	Formation of a protective SiO mask for ionic and plasma-chemical field etching of NbN-Au
<i>g</i>	Ionic and plasma-chemical field etching of NbN-Au

antenna interior allowed to control contact resistance of the NbN HEB mixers with the antenna. Before deposition of the NbN film, the Si substrate with orientation 100 was cleaned in oxygen plasma during 5 min at 150 W with following etching in HF:H₂O (1:30) during 30 s. The substrate temperature during deposition could vary from 25 to 350–450°C. Optimum thickness, critical temperature T_c and critical current density j_c were obtained with the following NbN deposition process parameters: substrate temperature — 400°C, partial pressures of Ar and N₂ — $5 \cdot 10^{-3}$ and $8-12 \cdot 10^{-5}$ mbar, respectively, discharge current and voltage — 300 mA and 300 V. NbN deposition after substrate cooling to 300°C was followed by *in situ* application of the Au layer. The NbN film deposition rate at the defined process specifications depended on the measurement of relation between film thickness that sputtering time. Like the NbN film thickness, the Au thickness was controlled by the deposition time on the basis of obtained deposition rates. Stages of quasi-optical NbN HEB mixer manufacturing stages are shown in detail in Figure 1 and in Table 1.

Typical dimensions of bolometers or superconducting bridges of the NbN HEB mixers varied within 0.1–0.4 μm in length and 1–4 μm in width. SEM photograph of the central part of the spiral antenna is shown in Figure 2.

With normal resistance per NbN film square $R_{\square} = 500-600 \Omega/\square$ (at NbN thickness of 3.5–4 nm), the bolometer length-to-width ratio L/W was equal to 10. Figure 2 shows the colored SEM photograph and schematic image of the NbN HEB mixer section. The mixer is composed of superconducting NbN film connected to Au ports of the planar antenna on the dielectric Si substrate. The detector design includes the open part of NbN film between the antenna arms — NbN bridge with set width W and length L and two-layer structure of the NbN/Au antenna

port. The NbN film under and near the Au contact has a lower critical temperature $(T_c)_2$ than the NbN bridge $(T_c)_1$.

2. DC measurements

DC measurements included the measurements of the NbN HEB mixer resistance vs. temperature $R(T)$, critical current j_c , residual resistance R_{res} . The NbN HEB mixer was installed in a copper holder at the end of an immersed helium insert made from stainless steel and placed into STG 40 Dewar vessel. The NbN HEB mixer resistance was measured in a four-point pattern using a precision low-noise stable current source and Solartron microvoltmeter. The four-point pattern is used to exclude lead wire resistance from the measurements. The temperature was measured by a calibrated diode silicon thermometer attached to the holder as close to the specimen as possible in such a way as its temperature was equal to the specimen temperature.

Due to cleaning of the Si substrate surface, specimens with $(T_c)_1$ spread of max. 0.15 K. For comparison, the *in situ* process without special surface preparation describe herein gives $(T_c)_1$ spread of about 1 K. Figure 3 shows the family of $R(T)$ specifications of the NbN HEB mixers made using the optimized route. The obtained proximity of $(T_c)_1$ for the prepared set suggests that they can operate as a single direct detector with a single common physical temperature or as a heterodyne detector with the same heterodyne power at each pixel inlet. In the early studies, the NbN film under the metal of antenna Au ports was cleaned in Ar- and O₂-plasma [5]. This process minimized the contact resistance between NbN and Au and limited the spread of normal resistances of the detectors with set L/W to the minimum value of max. 2 Ω. The study uses, instead of contact cleaning, 20 nm Au layer deposited *in situ* with the

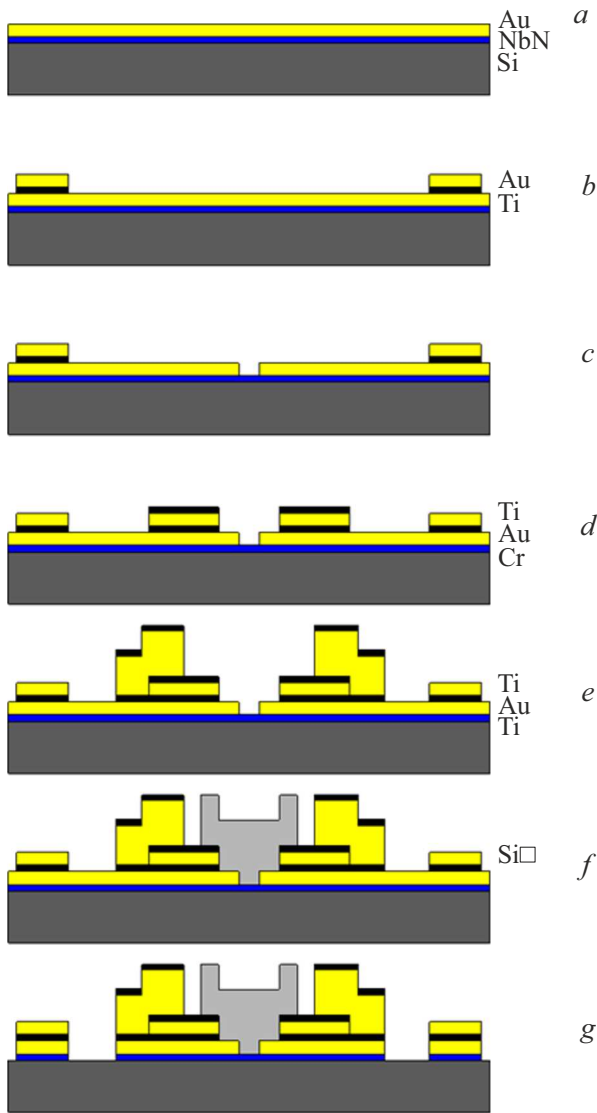


Figure 1. Stages of quasi-optical NbN HEB mixer manufacturing process. Explanations for the content of stages in Table 1.

NbN film — contact with the planar THz antenna. Quality of the electric contact between NbN and Au explains the appearance of the second junction on $R(T)$ due to the proximity effect. NbN HEB resistance at $(T_c)_1 < T < (T_c)_2$ is integrated into the superconducting NbN bridge and is provided by the conversion of the normal electron current at a length approximately equal to the coherency length ξ into the Cooper pair current, its value is defined by W , ξ and surface resistance of the NbN film at T slightly higher than $(T_c)_1$.

$(T_c)_2$ of the HEB mixer indirectly indicates a thickness of the deposited NbN film. Besides the additional resistance, the charge carrier conversion process results in coordinate dependence of the order parameter at T near $(T_c)_1$, which may result in smearing of the superconducting transition of the NbN bridge, increase in $\Delta(T_c)_1$, and finally reduces dR/dT of the detector. Thus, for HEB made without

cleaning NbN under the metal of Ti/Au ports of the antenna, the second transition was absent and $\Delta(T_c)_1$ was 0.2–0.3 K compared with $\Delta(T_c)_1$ 1.5–2 K for samples prepares using cleaning and *in situ* process. In this case, the specimens made without cleaning had high contact resistance about 25–30 Ω and, therefore, had much higher noise temperature.

Figure 4 shows the CVC family of detector 2026_2#9 for the set of substrate temperatures from 5 K to $T > (T_c)_1$ of the NbN HEB mixer. Figure 4 may be also interpreted as the evolution of characteristic IV of HEB in transition from S/SS'-state when the NbN bridge and NbN/Au layer of the antenna are in the superconducting state to the NSN state

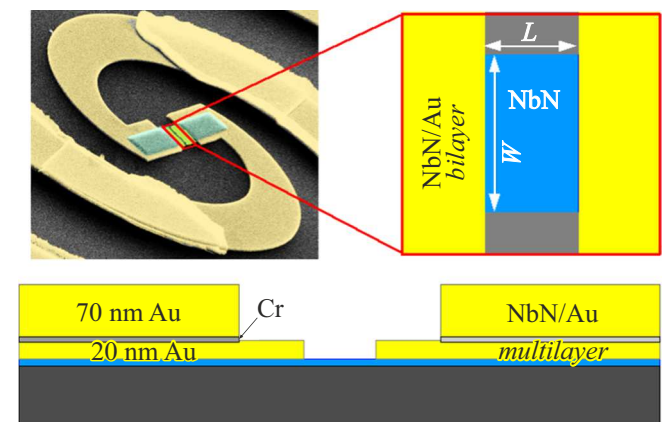


Figure 2. Appearance of the NbN HEB-mixer integrated into the planar spiral antenna. Arrangement of the layers composing the mixer interior, NbN and Au film interfaces of the planar antenna.

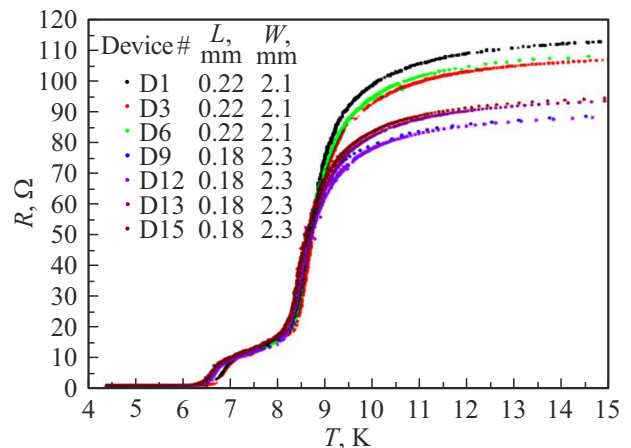


Figure 3. $R(T)$ characteristics of the HEB mixers made by *in situ* technique with Au on the prepared Si substrate. Superconducting transition near 8.5 K belongs to the NbN film in the bridge center between interfaces. The second transition belongs to the NbN film under the *in situ* Au of the antenna. Resistance after the first transition suggests the presence of two suppressed superconductivity regions in the NbN bridge near the normal metal (*in situ* Au) of the antenna, the length of these regions is approximately equal to the coherency length at the set T .

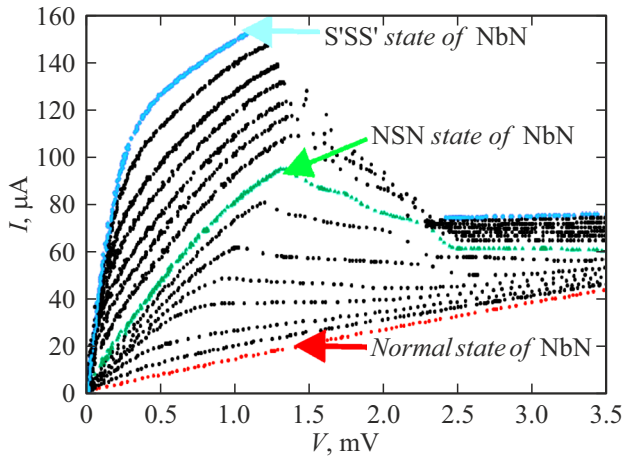


Figure 4. CVC evolutions of the NbN HEB mixer in transition from S'SS'-state when the NbN bridge and two-layer NbN/Au contact are in the superconducting state to the NSN-state when the NbN bridge is still superconducting and the two-layer NbN/Au contacts are already in normal condition.

when the NbN bridge is superconducting and the NbN/Au layer of the antenna is in normal state [8].

3. Noise temperature measurements

Noise temperature was measured at the heterodyne frequency of 2.52 THz using the „cold“/„hot“ (77 K/300 K) absolutely black body. submillimeter water vapor laser at 2.52 THz was used as the heterodyne radiation source.. At the mixer inlet, the heterodyne radiation power was controlled by a motor-operated quasi-optical polarizer formed by a metal grid with $25 \times 500 \mu\text{m}$ mesh. using a $3.5 \mu\text{m}$ mylar beam divider, the heterodyne radiation was combined with the black-body radiation. „Ecosorb“ was used as a black body. Transmittance of the beam divider was 97% at 2.52 THz.

The radiation was introduced into the helium cryostat through the 50 mm window made from 0.2 mm HDPE. The window transmittance was 80%. After the IR filter from Zitex 106 attached to the cryostat nitrogen screen and the bandpass IR mesh filter on the helium screen, the radiation fell onto an elliptical silicon lens. The mesh filter was made from Ni mesh with a period of $100 \mu\text{m}$. The total transmittance of the filter system was 90%. The elliptical lens used in the setup had no antireflection coating, therefore, it induced additional reflection loss of about 25% due to the difference of silicon–vacuum refraction indices. Using the elliptical lens of 10 mm in diameter, radiation was collected into the Airy spot on the planar antenna of the mixer. The lens with the mixer was secured in the mixing unit thermally connected to the cold plate of the helium cryostat. The mixing unit was made from oxygen-free copper. The planar antenna of the mixer blended smoothly into the 50 Ohm coplanar

line. The intermediate frequency (IF) signal was removed using a flexible 50 Ohm coplanar line with SMA high-frequency outlet connector. Then the IF signal arrived to the offset adapter with 1–10 GHz band. The adapter was used to provide DC offset of the specimen in the voltage generator mode and to transmit the IF signal to the cooled amplifier input, noise temperature within 1–7 GHz was maximum 10 K. The IF signal was output from the cryostat via the coaxial line and additionally amplified by a stage at room temperature. Secondary amplification used two types of amplifiers optimized to different frequency bands depending on the problem to be solved. After the first „warm“ amplifier, the signal passed through the adjustable bandpass filter with a bandwidth of 50 MHz and variable bandwidth of 1–10 GHz. The output power of IF was measured using a square-law semiconductor detector with a volt-watt sensitivity of 1000 V/W, the signal from the detector was recorded by the microvoltmeter and processed using the fast Fourier transform algorithm. The cold load radiation was simulated by the room temperature load at 12.5 Hz. For high temperatures and low frequencies in the Rayleigh–Jeans approximation when the spectral density of the black body is proportional to its physical temperature, the noise temperature is calculated through the Y -factor using equation

$$T_n = (T_{hot} + T_{cold} \cdot Y)/(Y - 1),$$

where T_{hot} and T_{cold} are the hot and cold load temperatures, respectively, Y is used to express Y -factor that is equal to the ratio of the mixer output power with input hot load to the mixer output power at cold load. Y -factor in case of the modulation measurement technique is defined from the Fourier transform spectrum as

$$Y = (U_- + K \cdot U)/(U_- - K \cdot U),$$

where U_- is the detector voltage at zero frequency, U is the detector voltage at modulation frequency, K is defined by the signal shape. At square-wave pulses, i.e. when the mixture aperture is much lower than the modulator blade, $K = \pi/4$. In a more general case, when the pulse ratio is 0.5, K is defined as the ratio of the Fourier's series first harmonic amplitude to the pulse amplitude.

Heat radiation power in noise temperature measurements applied to the mixer inlet from the black-body load in the Rayleigh–Jeans approximation is proportional to the load temperature and receiver input bandwidth:

$$P_{load} = k_B \cdot T \cdot \Delta F,$$

where k_B is the Boltzmann constant, T is the load temperature, ΔF is the receiver input bandwidth. This heat radiation, if ΔF is not limited in a special way, may cause bolometric response of the mixer when „hot“ and „cold“ input loads are changed. The bolometric response results in the shift of the mixer operating point on CVC synchronously with the input load change, that in turn causes the change in

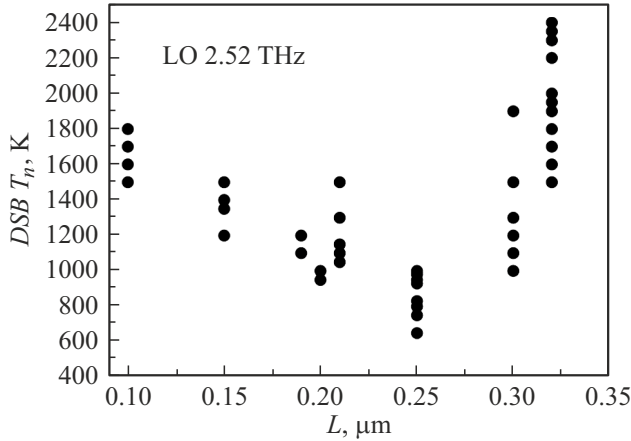


Figure 5. Dependence of the noise temperature of the NbN HEB mixer on the NbN bridge length measured at the heterodyne frequency of 2.52 THz. The mixers with the bridge length of 0.25 μm were made using the optimized process route. The measured noise temperature spread with mean value 800 K was maximum 150 K.

the conversion ratio and variation of the mixer output noise unproportional to the load temperature. This effect is called as the direct detection effect. When measuring the noise temperature of the mixer, this effect has a negative impact because it distorts the measured Y -factor. A cooled narrow-bandwidth filter used in the system almost avoided direct detecting and reduced its effect on the noise temperature measurements to lower than 5%.

As mentioned above, the optical path of the mixer consists of a polyethylene window, Zitex 106 broadband IR filter, narrow-bandwidth Ni mesh filter and elliptical silicon lens. The path components have loss L (times), and the equivalent noise temperature of the component with loss L at physical temperature T may be written as:

$$T_{equiv} = T_{CW}(T) \cdot (L - 1),$$

where $T_{CW}(T)$ is the equivalent temperature of the black body that has temperature T calculated by the Callen–Welton theorem [16]:

$$T_{CW}(T) = (hf/k_B)/(\exp(hf/k_B T) - 1) + hf/2k_B,$$

where h is the Planck's constant, k_B is the Boltzmann constant, T is the physical temperature, f is the heterodyne frequency. At relatively low frequencies f and high temperatures T , $T_{CW} \approx T$, and the expression for the equivalent noise temperature may be written as $T_{equiv} = T \cdot (L - 1)$. Table 2 shows the measured loss factors, physical temperatures and calculated equivalent noise temperatures of the optical path components of the mixer.

The nameplate noise temperature of the cold amplifier at 15 K is equal to 8–10 K in the amplifier operating bandwidth. The noise temperature of the total IF cold path, including the magnetic gate with 50 Ohm load, offset adapter and amplifier, is about 35 K. Taking into account the

cold amplifier gain of 35 dB, the IF path noise temperature may be neglected.

Thus, the total optical path loss was 3.17 dB with equivalent noise temperature 96.6 K.

To estimate intrinsic conversion loss of the mixer during the experiment, the U -factor was measured. The U -factor is numerically equal to the ratio of output noise when the mixer is in the operating point with 300 K input load to the output noise when the mixer is in the superconducting state, in this case the amplifier is loaded to the 50 Ohm gate load. Expression for the U -factor may be written as:

$$U = (T_{out} + T_{IF} + T_{load})/(T_{load} + T_{IF}),$$

where $T_{out} = (T_n)_{mix} + T_{300}^* \eta$, $(T_n)_{mix}$ are intrinsic noise, η is the total conversion loss of the mixer. T_{IF} is the noise temperature of the „cold“ amplifier, T_{load} is the 50 Ohm load temperature. From the expression for the U -factor, the internal noise temperature of the mixer can be expressed:

$$(T_n)_{mix} = U(T_{load} + T_{IF}) - (T_{IF} + T_{load} + T_{300}^* \eta).$$

Total conversion loss of the mixer are calculated as a ratio noise temperature calculated in terms of the U -factor to the measured noise temperature of the mixer

$$\eta = (T_n)_{mix}/T_{res}.$$

50 Ohm load of the circulator was at $T_{load} = 4.2$ K, noise temperature of the „cold“ amplifier was assumed equal to $T_{IF} = 10$ K. $T_{res} = 800$ K and the U -factor equal to 3 were calculated in the experiment with mixer 1178/1 #21 at the heterodyne frequency 2.5 THz. Thus, the total conversion loss η of mixer 1178/1 #21 is equal to 16.5 dB. Taking into account the optic loss of 3.17 dB, the intrinsic conversion loss is 13.3 dB.

The investigation of the fabricated NbN HEB mixers at 4.5 K in S'SS' state demonstrate the noise temperature at the heterodyne frequency of 2.52 THz, T_n 800 K with spread 150 K, and the mixer noise bandwidth was 7 GHz. Figure 5 shows the experimental dependence of the noise temperature of the *in situ* mixer on the NbN bridge width. Quite large noise temperature spread of about 1000 K for specimens from the same batch made using the non-optimized film deposition and mixer manufacturing route (with the same NbN bridge width) may be explained by the NbN film thickness inhomogeneity on the substrate and by the process influence on the NbN film during the mixer manufacturing process. Figure 5 also shows that the dependence has a clearly expressed valley. Unlike the *ex situ* mixers, as the NbN bridge width is decreased, the noise temperature of the test mixers decreases. This continues up to the bridge width of 0.25 μm , at this length the minimum noise temperature of the mixer was 600 K, this batch was made using the optimized technique. The noise temperature dependence trend in the NbN bridge width area more than 2 μm may be explained in terms of the theory of homogeneous heating in superconductor.

Table 2. Loss factors, physical temperatures and equivalent noise temperatures of the optical path components of the mixer

Optical path component	Loss factor L , dB	Physical temperature T , K	Noise temperature T_{equiv} , K
Beam divider	0.3	300	21.5
cryostat window(HDPE)	0.9	300	69.1
Zitex IR filter 106	0.22	77	4
Bandpass mesh	0.25	4.2	0.25
Silicon lens	1.5	4.2	1.73

Because the heat removal factor G included in the Johnson noise and thermodynamic fluctuation noise expressions is in square-law dependence on the NbN bridge width, its decrease shall result in reduction of the noise temperature of the mixer, which may be seen in the right-hand part of the curve. This suggests that the *in situ* mixers have no noise temperature limits attributed to the contact resistance.

With further reduction of the NbN bridge width and, thus, of its length, the noise temperature of the mixer starts growing. Based on the theory representations the noise temperature shall decrease with the width and, thus, with the bridge volume by the law which is close to that shown in the right-hand part of the curve. Sharp increase in the noise temperature when the bridge width less than $2\ \mu\text{m}$ is achieved is not described in terms of the theory of homogeneous electron heating in superconductors. Growth of the noise temperature is possibly caused by the increase in the contact resistance between the bridge and planar antenna ports due to the contact area reduction. This result may be used as one of the contact quality criteria for the *in situ* HEB mixer manufacturing process. The second, more probable, explanation is in that the bridge length with its width approaches the diffusion length in NbN. In this case the electron that has absorbed a high-energy photon without interaction with other electron goes to the bulk metal contact without changing the electronic temperature in the bridge. And the excited electron is not involved in the mixer response to the signal emission. If this assumption is true, then, besides the useful signal loss, operation of the additional diffusion cooling channel of the electronic subsystem shall also affect the required heterodyne power. Anyhow, this issue is of research interest and requires further targeted and more detailed investigations.

Conclusion

The study has experimentally defined optimum parameters of NbN film deposition to obtain 4–5 nm films and the Si substrate cleaning condition. Au layer *in situ* deposition with NbN film deposition ensured a stable and low-resistance electric contact. The absence of a barrier at the NbN/Au interface suggests the appearance of the second

superconductor transition depending on the $R(T)$ NbN HEB mixers, in addition, the NbN HEB mixers made from the same NbN film has almost identical $R(T)$. This ensures the same required heterodyne power and offset voltage for the specimens with identical dimensions L and W . The optimum L and W of the NbN bridge with respect to the noise temperature were 0.25 and $2.5\ \mu\text{m}$. The noise temperature of such NbN HEB mixers measured at the heterodyne frequency of 2.52 THz had a mean value of 800 K with spread 150 K. Noise bandwidth of mixers at $T = 4.5\ \text{K}$ was equal to 7 GHz. The intrinsic conversion loss at 1.5 GHz is 13.3 dB.

Funding

Manufacturing and testing of the HEB mixers were performed under grant № 23-12-00187 provided by the Russian Science Foundation. The literature on the subject of research was reviewed under the project of universities involvement in the development of high-technology production supported by the Ministry of Science and Higher Education of the Russian Federation (Agreement dated 06.04.2022 № 075-11-2022-026).

Conflict of interest

The authors declare that they have no conflict of interest.

References

- [1] H.M. Pickett, R.L. Poynter, E.A. Cohen, M.L. Delitsky, J.C. Pearson, H.S.P. Muller. *J. Quant. Spectrosc. Radiat. Transfer*, **60**, 883 (1998). DOI: 10.1016/S0022-4073(98)00091-0
- [2] P.L. Richards, T.M. Shen, R.E. Harris, F.L. Lloyd. *Appl. Phys. Lett.*, **34**, 345 (1979). DOI: 10.1063/1.90782
- [3] G.J. Dolan, T.G. Phillips, D.P. Woody. *Appl. Phys. Lett.*, **34**, 347 (1979). DOI: 10.1063/1.90783
- [4] A. Karpov, D. Miller, J.A. Stern, B. Bumbl, H.G. LeDuc, J. Zmuidzinas. *Proc. 19th int. Symp. on Space Terahertz Technology* (Groningen, The Netherlands, 2008), p. 68.
- [5] I. Tretyakov, S. Ryabchun, M. Finkel, A. Maslennikova, N. Kurova, A. Lobastova, B. Voronov, G. Gol'tsman. *Appl. Phys. Lett.*, **98**, 033507 (2011). DOI: 10.1063/1.3544050

- [6] *SOFIA — Stratospheric Observatory for Infrared Astronomy*. <http://www.sofia.usra.edu>.
- [7] Th. de Graauw, F.P. Helmich, T.G. Phillips, J. Stutzki, E. Caux, N.D. Whyborn, P. Dieleman, P.R. Roelfsema, H. Aarts, R. Assendorp, R. Bachiller, W. Baechtold, A. Barcia, D.A. Beintema, V. Belitsky, A.O. Benz, R. Bieber, A. Boogert, C. Borys, B. Bumble, P. Cais, M. Caris, P. Cerulli-Irelli, G. Chattopadhyay, S. Cherednichenko, M. Ciechanowicz, O. Coeur-Joly, C. Comito, A. Cros, A. de Jonge, G. de Lange, B. Delforges, Y. Delorme, T. den Boggende, J.-M. Desbat, C. Diez-González, A.M. Di Giorgio, L. Dubbeldam, K. Edwards, M. Eggens, N. Erickson, J. Evers, M. Fich, T. Finn, B. Franke, T. Gaier, C. Gal, J.R. Gao, J.-D. Gallego, S. Gauffre, J.J. Gill, S. Glenz, H. Golstein, H. Goulooze, T. Gunsing, R. Güsten, P. Hartogh, W.A. Hatch, R. Higgins, E.C. Honingh, R. Huisman, B.D. Jackson, H. Jacobs, K. Jacobs, C. Jarchow, H. Javadi, W. Jellema, M. Justen, A. Karpov, C. Kasemann, J. Kawamura, G. Keizer, D. Kester, T.M. Klapwijk, Th. Klein, E. Kollberg, J. Kooi, P.-P. Kooiman, B. Kopf, M. Krause, J.-M. Krieg, C. Kramer, B. Kruiuzenga, T. Kuhn, W. Laauwen, R. Lai, B. Larsson, H.G. Leduc, C. Leinz, R.H. Lin, R. Liseau, G.S. Liu, A. Loose, I. López-Fernandez, S. Lord, W. Luinge, A. Marston, J. Martín-Pintado, A. Maestrini, F.W. Maiwald, C. McCoe, I. Mehdi, A. Megej, M. Melchior, L. Meinsma, H. Merkel, M. Michalska, C. Monstein, D. Moratschke, P. Morris, H. Muller, J.A. Murphy, A. Naber, E. Natale, W. Nowosielski, F. Nuzzolo, M. Olberg, M. Olbrich, R. Orfei, P. Orleanski, V. Ossenkopf, T. Peacock, J.C. Pearson, I. Peron, S. Phillip-May, L. Piazzo, P. Planesas, M. Rataj, L. Ravera, C. Risacher, M. Salez, L.A. Samoska, P. Saraceno, R. Schieder, E. Schlecht, F. Schlöder, F. Schmö lling, M. Schultz, K. Schuster, O. Siebertz, H. Smit, R. Szczerba, R. Shipman, E. Steinmetz, J.A. Stern, M. Stokroos, R. Teipen, D. Teyssier, T. Tils, N. Trappe, C. van Baaren, B.-J. van Leeuwen, H. van de Stadt, H. Visser, K.J. Wildeman, C.K. Wafelbakker, J.S. Ward, P. Wesselius, W. Wild, S. Wulff, H.-J. Wunsch, X. Tielens, P. Zaal, H. Zirath, J. Zmuidzinas, F. Zwart. *A& A*, **518** (L6), 7 (2010). DOI: 10.1051/0004-6361/201014698
- [8] P. Putz, C.E. Honingh, K. Jacobs, M. Justen, M. Schultz, J. Stutzki. *A& A*, **542** (L2), 5 (2012). DOI: 10.1051/0004-6361/201218916
- [9] C. Risacher, R. Gusten, J. Stutzki, H.W. Hubers, D. Buchel, U.U. Graf, S. Heyminck, C.E. Honingh, K. Jacobs, B. Klein, T. Klein, C. Leinz, P. Putz, N. Reyes, O. Ricken, H.J. Wunsch, P.M. Fusco, S.W. Rosner. *IEEE Trans. THz Sci. Technol.*, **6** (2), 199 (2016). DOI: 10.1109/TTHZ.2015.2508005
- [10] S.-C. Shi, S. Paine, Q.-J. Yao, Z.-H. Lin, X.-X. Li, W.-Yi. Duan, H. Matsuo, Q. Zhang, Ji Yang, M.C.B. Ashley, Zh. Shang, Zh.-W. Hu. *Nature Astronomy*, **1** (1), (2017). DOI: 10.1038/s41550-016-0001
- [11] Proekt Millimetron. <http://www.asc.rssi.ru/millimetron/rus/millim.htm>
- [12] N.S. Kardashov, I.D. Novikov, V.N. Lukash, S.V. Pilipenko, E.V. Mikheeva, D.V. Bisikalo, D.Z. Vibe, A.G. Doroshkevich, A.V. Zasov, I.I. Zinchenko, P.B. Ivanov, V.I. Kostenko, T.I. Larchenkova, S.F. Likhachev, I.F. Malov, V.M. Malofeev, A.C. Pozanenko, A.V. Smirnov, A.M. Sobolev, A.M. Cherepashchuk, Yu.A. Shchekinov. *UFN*, **184**, 1319 (2014). DOI: 10.3367/UFNe.0184.201412
- [13] I. Tretyakov, S. Ryabchun, M. Finkel, A. Maslennikova, N. Kaurova, A. Lobastova, B. Voronov, G. Gol'tsman. *Appl. Phys. Lett.*, **98**, 033507 (2011). DOI: 10.1063/1.3544050
- [14] M. Shcherbatenko, I. Tretyakov, Yu. Lobanov, S.N. Maslennikov, N. Kaurova, M. Finkel, B. Voronov, G. Goltsman, T.M. Klapwijk. *Appl. Phys. Lett.*, **109**, 132602 (2016). DOI: 10.1063/1.4963691
- [15] J.J.A. Baselmans, M. Hajenius, J.R. Gao, T.M. Klapwijk, P.A.J. de Korte, B. Voronov, G. Gol'tsman. *Appl. Phys. Lett.*, **84**, 1958 (2004). DOI: 10.1063/1.1667012
- [16] H.B. Callen, Th.A. Welton. *Phys. Rev.*, **83**, 34 (1951). DOI: 10.1103/PhysRev.83.34

Translated by E.Iinskaya